‘Sarcomeres’ of smooth muscle: functional characteristics and ultrastructural evidence

Ana M. Herrera[1,3], Brent E. McParland[3], Agnes Bienkowska[3], Ross Tait[3], Peter D. Paré[2,3] and Chun Y. Seow[1,3,*]

[1]Department of Pathology and Laboratory Medicine, [2]Department of Medicine and [3]James Hogg iCAPTURE Centre for Cardiovascular and Pulmonary Research, St Paul’s Hospital/Providence Health Care, University of British Columbia, 1081 Burrard Street, Vancouver, BC V6Z 1Y6, Canada

*Author for correspondence (e-mail: cseow@mrl.ubc.ca)

Accepted 9 March 2005
Journal of Cell Science 118, 2381-2392 Published by The Company of Biologists 2005
doi:10.1242/jcs.02368

Summary

Smooth muscle cells line the walls of hollow organs and control the organ dimension and mechanical function by generating force and changing length. Although significant progress has been made in our understanding of the molecular mechanism of actomyosin interaction that produces sliding of actin (thin) and myosin (thick) filaments in smooth muscle, the sarcomeric structure akin to that in striated muscle, which allows the sliding of contractile filaments to be translated into cell shortening has yet to be elucidated. Here we show evidence from porcine airway smooth muscle that supports a model of malleable sarcomeric structure composed of contractile units assembled in series and in parallel. The geometric organization of the basic building blocks (contractile units) within the assembly and the dimension of individual contractile units can be altered when the muscle cells adapt to different lengths. These structural alterations can account for the different length-force relationships of the muscle obtained at different adapted cell lengths. The structural malleability necessary for length adaptation precludes formation of a permanent filament lattice and explains the lack of aligned filament arrays in registers, which also explains why smooth muscle is ‘smooth’.

Key words: Isotonic shortening, Plasticity, Contraction mechanism, Length adaptation, Ultrastructure

Introduction

The ability of smooth muscle to shorten is the most important attribute that allows the tissue to carry out its physiological function, and any abnormal enhancement or diminution in the shortening capability invariably leads to dysfunction of the organ concerned. The sliding-filament, crossbridge mechanism of contraction developed for skeletal muscle (Hanson and Huxley, 1953; Huxley and Niedergerke, 1954; Huxley, 1957) is also believed to be responsible for smooth muscle contraction (Guilford and Warshaw, 1998). Sarcomeres of striated muscle have been well characterized in terms of their structure and function (Gordon et al., 1966), the equivalent basic contractile units in smooth muscle, however, are still poorly understood. Structural evidence suggests that the myosin thick filament in smooth muscle is either side-polar (Small, 1977; Cooke et al., 1987; Xu et al., 1996; Tonino et al., 2002), or row-polar (Hinssen et al., 1978), with 14-15 nm periodicity along the entire filament length and no central bare zone (devoid of crossbridges), in contrast to the bipolar thick filaments found in striated muscle that possess a central bare zone. If indeed the thick filaments in smooth muscle are not bipolar, the contractile unit structure will necessarily be different from the sarcomere structure of striated muscle. The structural difference will in turn confer unique functional characteristics on smooth muscle. In the present study, a model of contractile unit is proposed to account for the unique length-force relationship observed in airway smooth muscle.

The ability of airway smooth muscle (Pratusevich et al., 1995; Gunst et al., 1995) and probably other smooth muscles (Uvelius, 1976; Gillis et al., 1988) to adapt to changes in length and maintain maximal force generation over a large length range appears to require plastic changes in subcellular structures that involves rearrangement of contractile units within the contractile apparatus and reshaping of the apparatus itself. Rearrangement of the contractile units due to length adaptation is modeled in the present study to account for the observed length-dependent changes in ultrastructure and mechanical properties.

Materials and Methods

Tissue preparation and apparatus of measurement

The apparatus and tissue preparation have been described previously (Herrera et al., 2002; Herrera et al., 2004). Porcine tracheal smooth muscle (trachealis) was used for the experiments. The tracheas were obtained from a local abattoir. The parallel in situ arrangement of trachealis cells in a bundle and low resting tension made the preparation ideal for this study. After removal from the animals, the tracheas were placed in physiological saline solution (PSS) at 4°C. In situ length ($L_{\text{in situ}}$) of a trachealis strip from one cartilage attachment to the other was measured before the C-shaped cartilage was cut. Attention was paid to the appearance of the epithelial-mucosal layer of the intact trachea: a wrinkled epithelial-mucosal layer usually

indicates contracted smooth muscle cells underneath. Any such trachea was discarded because the in situ length could not be accurately measured. A rectangular sheet of relaxed smooth muscle tissue at its in situ length, free of connective tissue, was dissected from the trachea. The piece of tissue was then cut into multiple strips along the longitudinal axes of the cell bundles; all the strips used in a single experiment had the same initial length as a result. The muscle preparations were ~11×1×0.3 mm in dimension. The strips of muscle were attached to aluminum foil clips at both ends and mounted in a muscle bath. One end of the strip was connected to a stationary hook and the other end to a length/force transducer (lever system) with a noise level of <0.1 mN and a compliance of ~1 μm/mN (QJin Design, Winnipeg, Canada). The computer-controlled lever system was able to measure muscle force either at a constant length (isometric force), or allow the muscle to shorten under a constant load (isotonic contraction), or apply a step change in length to the muscle at any predetermined time. A step change in length was completed in less than 100 milliseconds.

Before a trachealis preparation was ready for experiment, it was equilibrated for about 1 hour at a predetermined length (0.75, 1.0 or 1.5 $L_{\text{in situ}}$). During the equilibration period, the muscle was electrically stimulated periodically to produce 12-second tetani at 5-minute intervals. The preparation was considered equilibrated when it developed a stable maximal isometric tetanic force with negligible resting tension. Isotonic shortenings were all initiated in an isometric state, i.e. the muscle was stimulated isometrically and only when the developed active force reached the level of a preset isotonic load was the muscle allowed to shorten isotonically. During relaxation, the muscle was not allowed to lengthen beyond the preset isometric length. Stimulation of the muscle was provided electrically with a 60 Hz alternating current at a voltage (20 V) that elicited maximal response from the muscle preparations. The onset and duration of the stimulation were computer-controlled. The muscle bath contained PSS with pH 7.4 at 37°C and aerated with a gas mixture containing 5% CO_2/95% O_2. The PSS had a composition of 118 mM NaCl, 4.5 mM KCl, 1.2 mM NaH_2PO_4, 22.5 mM $NaHCO_3$, 2 mM $MgSO_4$, 2 mM $CaCl_2$ and 2 g/l dextrose.

Determination of the relationship between actively shortened muscle length and the associated active force

In an isotonic contraction (i.e. a contraction under constant load), a muscle will shorten dynamically until the system comes to a static mechanical equilibrium. Shortening stops when the static force generation of the muscle equals that of the applied load. This static force equilibrium occurs at the plateau of an isotonic contraction where the shortening velocity is zero. By applying different isotonic loads to the muscle, the corresponding shortened lengths (at plateaus) can be measured. In this study, a series of isotonic loads ranging from 10-90% of maximal isometric force (F_{max}) were applied to a muscle to obtain the corresponding maximally shortened lengths, and thus obtaining the length-force relationship for the muscle preparation.

In experiments where a quick stretch was applied to the muscle followed by an isotonic contraction, the quick length change was accomplished by the rotation of the servo lever to which the muscle was attached, using the step-length-change feature of the apparatus. The change in length occurred 10 seconds before stimulation of the muscle to allow the passive viscoelastic tissue response to settle. The maximal isometric force (F_{max}) obtained from a contraction immediately following a quick stretch was slightly lower than the F_{max} obtained without a quick stretch. For each preparation, the F_{max} post stretch was determined, and in the subsequent isotonic contraction, the isotonic load was calculated according to the post-stretch F_{max}.

Analysis of force-velocity and force-power relationships

In our experiments, the maximal rate of shortening occurred near the beginning of an isotonic contraction. For each isotonic load, we measured the maximal rate of shortening, and the pair of data constituted a force-velocity point. Five such points were obtained at isotonic loads that were 10, 30, 50, 70 and 90% of F_{max}. Because shortening velocity of smooth muscle is a function of both load and time (Dillon et al., 1981; Seow and Stephens, 1986), the force-velocity curve obtained with the present method did not represent the standard (or conventional) force-velocity relationship of the muscle owing to the fact that the velocities were measured at different times after stimulation. The reason that the velocities were measured at different times in the present study was because the onset of isotonic contraction was load-dependent, i.e. the greater the load, the later the onset. In this study, we were not interested in obtaining the standard force-velocity relationship of the muscle; we were interested in comparing the velocities of the same muscle adapted to different lengths.

Despite the fact that the force-velocity data from the present study were obtained under conditions where the time (after stimulation) variable was not constant, the data were well fitted with a hyperbolic function. The Hill's hyperbolic equation (Hill, 1938) was used to fit the data:

$$V = b(F_{\text{max}} - F)/(F + a),$$

where V is shortening velocity, F is isotonic load, and a and b are Hill's constants (Hill, 1938). A non-linear method (SigmaPlot® software) was used to perform the curve fitting. Velocity change in a muscle adapted to different lengths was determined by scaling velocity values of the force-velocity curve obtained at a reference length by a constant factor that produced the best fit for the force-velocity data obtained at the test length as described (Pratusevich et al., 1995). Muscle power output (P) as a function of load (F) was obtained by multiplying V and F,

$$P = FV = Fb(F_{\text{max}} - F)/(F + a).$$

Determination of the relationship between isotonic load and the amount of shortening in a muscle adapted to different lengths

In this group of experiments, we determined the length-force relationship of trachealis preparations that were equilibrated for about 1 hour at one of the two lengths: 1.5 times the in situ length ($L_{\text{in situ}}$), and 0.75 $L_{\text{in situ}}$. Six muscle preparations from six pigs were used for this group of experiments. Three of the muscle preparations were equilibrated at 0.75 $L_{\text{in situ}}$; the other three at 1.5 $L_{\text{in situ}}$. Five isotonic loads (as mentioned above) were used to generate a curve that described the relationship between the isotonic load and the corresponding maximal amount of shortening. At lighter loads (<50% F_{max}) maximal shortening was reached in less than 12 seconds of stimulation; at heavier loads, longer stimulation time (up to 27 seconds) was needed to obtain maximal shortening. It should be pointed out that the true plateau of an isotonic contraction may not be obtainable if there is ongoing adaptation of the muscle to length change. The protocol described above therefore excluded the effects of slow length adaptation that might occur in a prolonged contraction. For muscle preparations equilibrated at 1.5 $L_{\text{in situ}}$, the length-force relationship was first obtained with the muscle shortening (against the five isotonic loads, randomly applied) from the initial length of 1.5 $L_{\text{in situ}}$. The same preparations were then readapted at 0.75 $L_{\text{in situ}}$ until their isometric force reached a stable, maximal level. This process (called length adaptation) took about 30-40 minutes and consisted of six to eight isometric contractions (12-second tetani) elicited at 5-minute intervals. The length-force relationship was then obtained with the muscle shortening from 0.75 $L_{\text{in situ}}$ against five isotonic loads (10-90% F_{max} as before, the F_{max} however was that obtained at 0.75 $L_{\text{in situ}}$). In between isotonic contractions, at least one isometric contraction was elicited to determine the level of isometric force.

Shortening at low isotonic loads often resulted in a reduction in the isometric force of the subsequent isometric contraction. Several isometric tetani (at 5-minute intervals) were often required to bring the isometric force back to the initial level before the isotonic contraction was elicited. For the muscle preparations equilibrated at 0.75 $L_{in\ situ}$, the length-force relationships were obtained in the reversed order as that described for the preparations equilibrated at 1.5 $L_{in\ situ}$. That is, a length-force relationship was obtained first at 0.75 $L_{in\ situ}$, followed by readapting the same muscle preparation at 1.5 $L_{in\ situ}$ and then obtaining the length-force relationship for that length. Results from the two groups were not statistically different and were combined in the final analysis.

Electron microscopy (EM)

Muscle preparations were fixed for EM using a conventional protocol described previously (Herrera et al., 2002; Qi et al., 2002). Briefly, muscle preparations were fixed with the primary fixing solution (see below for details) for 15 minutes while they were still attached to the experiment apparatus. Care was taken not to physically perturb the tissue during the initial fixation. The tissue was then removed from the apparatus and cut into small cubes and immersed in the primary fixing solution for an additional 2 hours at 4°C. The primary fixing solution contained 2% glutaraldehyde, 2% paraformaldehyde and 2% tannic acid in 0.1 M sodium cacodylate buffer. In the process of secondary fixation, the small tissue cubes were put in 1% OsO_4 in 0.1 M sodium cacodylate buffer for 2 hours. The tissue was then stained with 1% uranyl acetate, dehydrated with increasing concentrations of ethanol and embedded in resin (TAAB 812 mix). The resin blocks were sectioned with a diamond knife to obtain sections of ~90 nm of thickness. The sections (on copper grids) were further stained with 1% uranyl acetate and Reynolds lead citrate. Images of thin sections of smooth muscle cells were obtain using a Phillips 300 electron microscope.

Morphometric and statistical analysis

Sampling and analysis were carried out 'blind'. The codes indicating experimental conditions were revealed only after the analysis of each group was finished. Specialized image analysis software (Image Pro-Plus 3.0) was used to help with the manual counting of the thick filaments by marking and keeping track of the number of filaments counted (tag-point counting). The software also helped in determining distance between two points and area measurements.

Statistical analysis and comparison among data groups were performed by one-way ANOVA or Student's *t*-test. For morphometric measurements, data from each animal were averaged first before the means from different animals were averaged. Values were expressed as mean±s.e.m. The level of statistical significance was set at $P<0.05$.

Results

Muscle cell length, contractile filament overlap and the ability to generate force

To interpret the relationship of overall muscle length and force generated by the muscle in terms of contractile filament overlap, one must make sure that the architecture of cell organization within the muscle preparation allows such interpretation. The highly parallel arrangement of a number of trachealis cells in longitudinal section (with their long axes aligned with the direction of force generation/transmission) was found to be a typical feature in all the micrographs examined at different magnifications (Fig. 1).

The relationship between muscle length and the ability of the muscle to generate force was examined (Fig. 2). For this group of experiments, muscle preparations were fully adapted at their in situ length ($L_{in\ situ}$) and all isotonic contractions started from $L_{in\ situ}$. The data points (filled circles) were obtained at the plateaus of contractions against isotonic loads of magnitudes 10-90% of the maximal isometric force (F_{max}). The average value for F_{max} (n=5) in this group was 154.5±12.2 (kPa). The length-force curve of skeletal muscle (Gordon et al., 1966) was plotted in the same figure (dotted lines) as a reference. The length-force data of the trachealis preparation (filled circles) were fitted with a straight line (solid).

The linear length-force relationship of trachealis can be explained by a simple model (Fig. 3). The model is similar to that proposed by Hodgkinson and colleagues (Hodgkinson et al., 1995) except that the thick filament is assumed to be as long as the distance between the dense bodies in a contractile unit and the thick filament completely overlaps the thin filaments. The contractile filament overlap will decrease as soon as the contractile unit shortens, and furthermore, the overlap decreases linearly as a function of the contractile unit length (Fig. 3). Ultrastructural evidence consistent with the

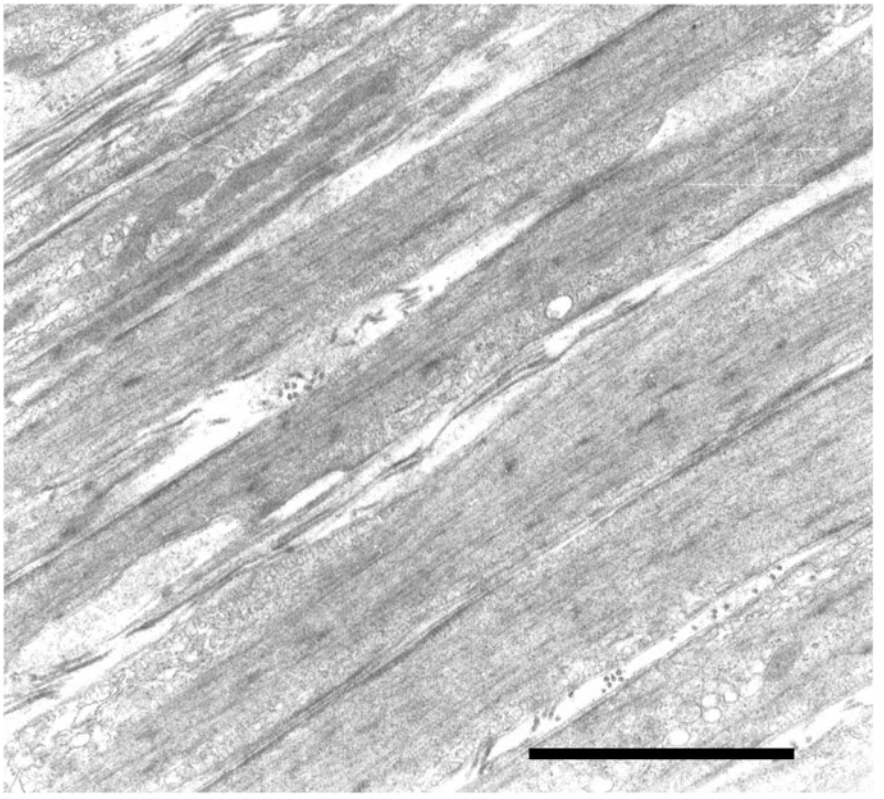

Fig. 1. Electron micrograph of a longitudinal section of a trachealis cell bundle fixed at the in situ length ($L_{in\ situ}$) in the relaxed state. Bar, 5 μm.

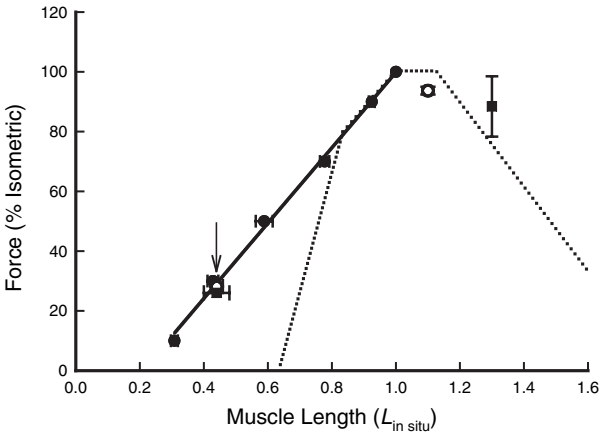

Fig. 2. The relationship between maximally shortened muscle length (normalized by the in situ length) and the isotonic load (expressed as a percentage of maximal isometric force). Solid circles are data obtained at plateaus of isotonic contractions under various loads and fitted with a linear line (solid). The dotted lines represent a reference length-force relationship from skeletal muscle [reproduced from Gordon et al. (Gordon et al., 1966)] with the sarcomere length of 2.0 μm superimposed on the in situ length of the trachealis. The open circles and filled squares are data obtained after quick stretches of magnitudes of 10% and 30% $L_{in\ situ}$, respectively, that show isometric forces at the stretched lengths and final shortened lengths (arrow) in isotonic contractions under a constant load of 30% F_{max}.

model can be found in trachealis cells (Fig. 4). The longitudinal sections shown (Fig. 4) however lack the resolution to confirm that thin filaments emanating from the relevant dense bodies interact with the thick filaments bracketed by the dense bodies.

The proposed model predicts that if a quick stretch is applied to the muscle just before it shortens, it will cause sliding of the thin and thick filaments relative to each other and create non-overlap zones between the filaments. The subsequent shortening will abolish these non-overlap zones and the final length to which the muscle shortens will be determined only by the applied load and not the prior stretch. This is graphically illustrated (Fig. 3C) and this model prediction was tested experimentally. A quick stretch of the amount of 10% $L_{in\ situ}$ was applied to muscles at their in situ length just before they were stimulated. Subsequent isometric contractions showed a ~6% decrease in F_{max} associated with the stretch (Fig. 2, open circle). Active shortening of the muscles under a load of 30% F_{max} resulted in a maximally shortened length that was not different from the one produced by muscles that were not subjected to a quick stretch (Fig. 2, open circle indicated by arrow). Repeating the experiment with a 30%-$L_{in\ situ}$ stretch prior to active shortening under a load of 30% F_{max} produced the same result in terms of the maximally shortened length (Fig. 2, filled square indicated by arrow, overlapping with open circle). The observations therefore are consistent with the model prediction.

If a quick stretch (applied to a relaxed muscle) results in an increase in the mean distance between dense bodies and creates non-overlap (thin filaments only) zones adjacent to the dense bodies (see Fig. 3C), we should be able to demonstrate this effect morphometrically. Fig. 5 shows a cell cross-section with contractile filaments and dense bodies. A magnified portion is shown in the inset. The number of thick filaments within a 60-nm perimeter surrounding the edge of a dense body was counted in cross-sections of three groups of trachealis cells: (1) fully adapted at the in situ length; (2) immediately after a quick stretch from $L_{in\ situ}$ to 1.3 $L_{in\ situ}$; (3) fully adapted at the stretched length of 1.3 $L_{in\ situ}$. Three trachealis preparations from three animals were used for this group of experiments. Six micrographs per condition per animal were used for the analysis; the total number of micrographs used in this group of experiments was therefore 54. The number of dense bodies identified was 548, 437, and 486 for the first, second and third group, respectively (Fig. 6). Immediately after the stretch, the thick filament density in the vicinity surrounding dense bodies decreased significantly by 29.1±3.4%, indicating that dense bodies were pulled away from some of the thick filaments during the quick stretch. This agrees with the force measurements (Fig. 2) and is consistent with the model (Fig. 3C). Full recovery of thick filament density was achieved after adaptation at 1.3 $L_{in\ situ}$ (Fig. 6). The adaptive behavior of the muscle is further described below.

Functional and structural changes after muscle adaptation to new lengths

Airway smooth muscle is known to adapt, in a time-dependent manner, to externally imposed changes in cell length (Pratusevich et al., 1995; Kuo et al., 2001). One of the outcomes of length adaptation appears to be optimization of contractile filament overlap that requires extensive reorganization of subcellular structures (Kuo et al., 2003). Most of the above-described experiments were designed to avoid length adaptation by using quick length changes followed by immediate measurement of mechanical properties or fixation for ultrastructural examination. The following group of experiments, in contrast, were designed to study the phenomenon of length adaptation; the muscle preparations were fully adapted after a length change. The gauge for the degree of adaptation after a length change was the extent of isometric force recovery. (See Materials and Methods for the protocol of length adaptation.)

Length-force relationships of trachealis preparations adapted to two lengths: 0.75 $L_{in\ situ}$ and 1.5 $L_{in\ situ}$ were determined (Fig. 7). Each preparation was studied in sequence at the two lengths. The relationship obtained at 1.0 $L_{in\ situ}$ (previously shown in Fig. 2) is shown here in gray as a reference. The linear feature of the relationship was retained at all lengths. The average value for F_{max} at 1.5 $L_{in\ situ}$ was 165.3±14.5 (kPa), no different from the F_{max} at 0.75 $L_{in\ situ}$; the ratio of (F_{max} at 1.5 $L_{in\ situ}$)/(F_{max} at 0.75 $L_{in\ situ}$) was 1.038±0.098 (n=6). (Note that the muscle preparations used to obtain the length-force relationship at 1.0 $L_{in\ situ}$ were from a separate group of experiments that used different tracheas.)

Force-velocity and force-power relationships of the same muscles adapted at 0.75 $L_{in\ situ}$ and 1.5 $L_{in\ situ}$ (whose length-force relationships are shown in Fig. 7) were calculated (Fig. 8). Hill's hyperbolic equation (Hill, 1938) was used to fit the force-velocity data obtained at 1.5 $L_{in\ situ}$ (Fig. 8, open circles and solid curve). For fitting the data obtained at 0.75 $L_{in\ situ}$ (filled circles), the solid hyperbolic curve was scaled down vertically by a factor of 0.61 (dashed curve). The increase in velocity at all loads with length doubling (from 0.75 to 1.5 $L_{in\ situ}$) was therefore 64% (1/0.61=1.64), a result very close to

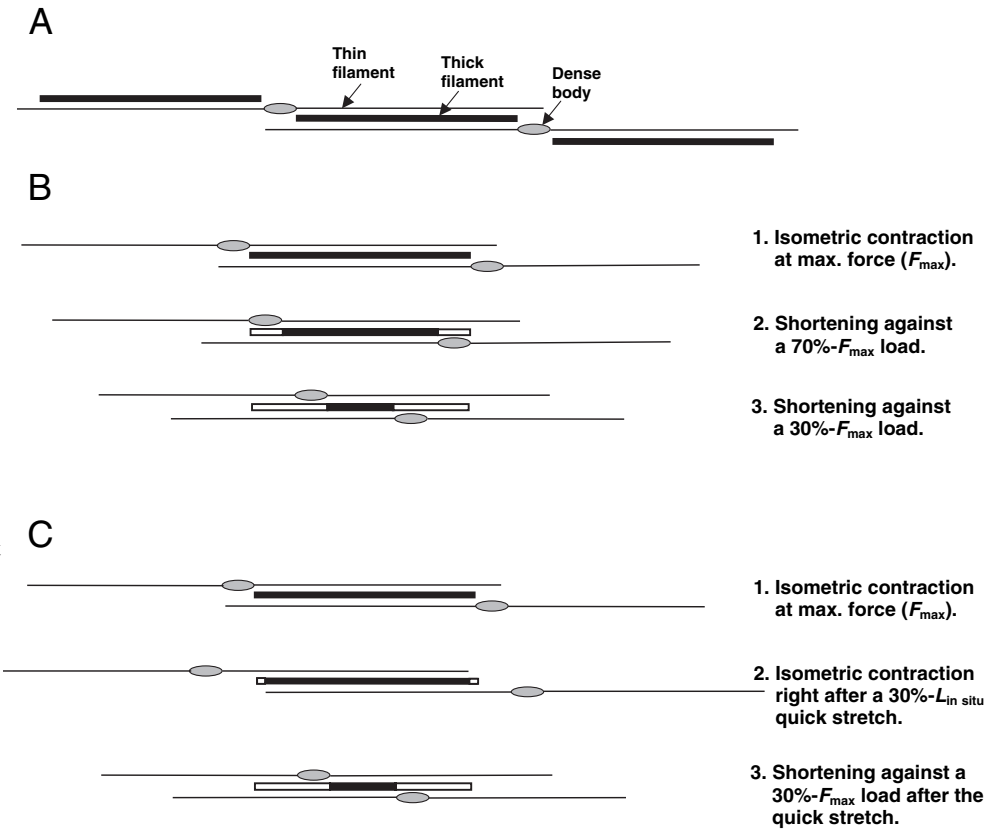

Fig. 3. Two-dimensional schematic representation of partial assemblies of contractile units in smooth muscle. (A) In a fully adapted muscle, the thick filaments are assumed to span the entire distance between the associated dense bodies. For simplicity, multiple attachments of thin filaments on one side of a dense body are not depicted. (B) Isometric contraction (1) and isotonic contractions (2,3) against different external loads. (C) Isometric contractions (1,2) at different lengths and isotonic contraction (3) against an isotonic load. Each numbered configuration represents an equilibrium (static) condition where external load equals the force produced by the contractile unit. The solid portion of the thick filaments represents the segment in between the dense bodies that overlaps with both of the thin filaments. It is assumed that only the cross bridges within the solid portion of the thick filaments can interact with the thin filaments properly to generate force. Length of the solid portion of the thick filaments in a contractile unit therefore correlates directly with the ability of the muscle to generate force or carry load during contraction. (See text for more details).

that found by others (Pratusevich et al., 1995). Because the maximal isometric force was not different at the two adapted lengths, the increase in power output with the increased adapted length was the same as the increase in velocity (Fig. 8).

The observed changes in force-velocity and force-power relationships (Fig. 8) due to length adaptation can be explained by a model where contractile units are added in series in muscles adapted to a longer length (Kuo et al., 2003). In fact, three variations of this model (Kuo et al., 2003) can all independently account for the changes in the force-velocity and force-power relationships induced by length adaptation (Fig. 9). All three models share the same features: an increase of 67% in the number of contractile units in series with a 100% increase in the adapted length. There are, however, differences among them that result in their very different predictions on the length-force relationship. The lower panel of Fig. 9 shows predictions from the three models superimposed on data redrawn from Fig. 7. Model C is the only one whose prediction agrees with experiment data.

The models incorporated extensive reorganization of the contractile apparatus in order to predict the changes after length adaptation; some of the structural changes can be verified by morphometric measurements. Results shown in Fig. 6 suggest that immediately after a quick stretch, non-overlap between thin and thick filaments could occur (seen as a decrease in the thick filament density surrounding the dense bodies, as a result of dense bodies being pulled away from the ends of thick filaments). However, after length adaptation, the non-overlap zones seemed to disappear, as suggested by the full recovery of thick filament density surrounding the dense bodies (Fig. 6). These results are consistent with Model B and C, but not A. Models A and B predict that the increase in the number of dense bodies per cell volume will be 67%; Model C predicts that the increase will be 33%. Morphometric measurements were carried out in muscle cells adapted at 0.75 and 1.5 $L_{in\ situ}$ (Fig. 10). Two tracheas were used. Eight micrographs (containing a longitudinal thin section of a cell) per length per animal were used; the total number of micrographs (or cells) used was therefore 32. The total number of dense bodies within each 4-μm segment was counted and divided by the area of the segment to obtain the density of the dense bodies (Fig. 11). The measured density increase of 34.0±13.2% was consistent with the 33% predicted by Model C, but very different from the 67% predicted by Models A and B.

Discussion

Our understanding of how striated muscle works has perhaps contributed to our belief that smooth muscle, like striated muscle, is composed of numerous contractile units arranged in series and in parallel. The serial arrangement of sarcomeres in a striated muscle cell amplifies the movement generated by each sarcomere and translates the microscopic conformational change in the myosin crossbridges into macroscopic shortening of the cell. Likewise, the parallel arrangement of sarcomeres allows the muscle cell to sum the forces generated by individual sarcomeres. The length of a contractile unit has to be small compared with the cell length; this is necessary to

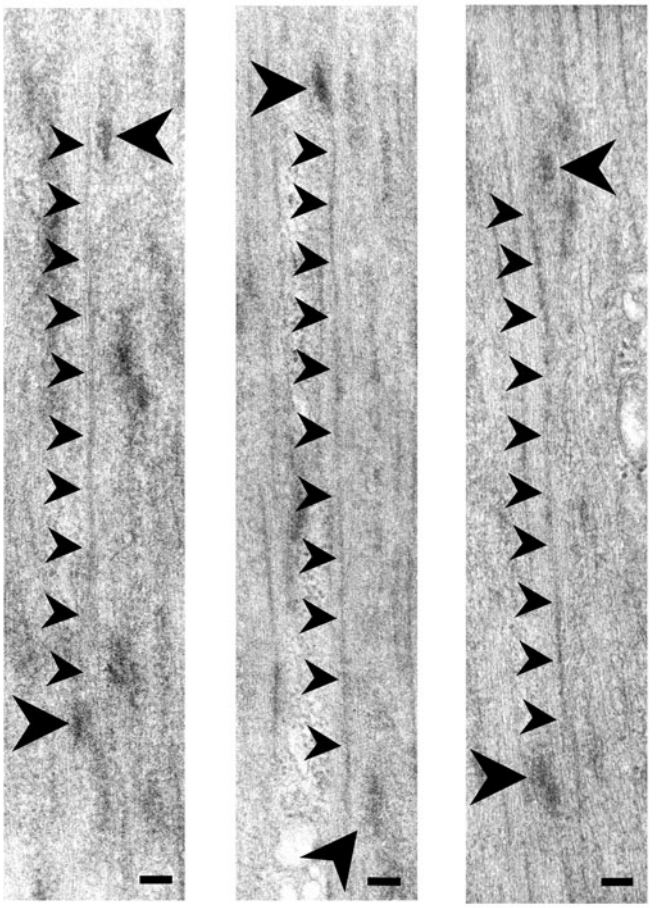

Fig. 4. Examples illustrating the spatial arrangement of myosin filaments and dense bodies that could be interpreted as a standard design of contractile unit in smooth muscle: a myosin filament spanning the distance between two dense bodies on opposite sides of the filament. The longitudinal EM sections were obtained from porcine trachealis fixed at their in situ length and in the relaxed state. Length of the thick filaments and the distance between the dense bodies are between 1.8-2.2 μm. Large arrowheads indicate the relevant dense bodies; small arrowheads follow the myosin thick filaments. Bar, 0.1 μm.

achieve a large amplification factor in shortening and velocity of shortening. In striated muscle, the ratio of cell length to sarcomere length is typically in the hundreds of thousands. Although the serial arrangement of contractile units in smooth muscle has never been clearly shown, the fact that the myosin crossbridges and their ATP-dependent conformational changes are responsible for smooth muscle shortening (Guilford and Warshaw, 1998) necessitates an arrangement that consists of a large number of contractile units in series and in parallel so that the effects of the microscopic movements in the contractile proteins can be adequately amplified.

Although the existence of contractile units in smooth muscle has a sound functional basis, there is no direct structural evidence. So far, we have relied on a few 'glimpses' of the ultrastructure for clues on how the contractile machinery of smooth muscle may be constructed. The seemingly random and certainly dynamic structure of the contractile filaments and the 'plastic' nature in the way they are assembled, features not found in striated muscle, are certainly factors responsible for the difficulty in our effort to understand smooth muscle ultrastructure and function. Results from the present study suggest that a thorough understanding of the mechanism of smooth muscle contraction will probably come from a combined knowledge of how individual contractile units work and how they are organized as a functional group. It is unlikely that we will ever find highly ordered contractile units (such as those depicted in the proposed models) in smooth muscle; the 'randomness' with which the contractile units appear to be organized may be a consequence of the need to adapt constantly to changes in cell length. One organizational feature that may have contributed to the random appearance is that the dense bodies are not lined up in cross-sections. Other features such as non-uniform filament lengths should also be kept in mind. In this report, the discussion of results is structured around the various proposed models.

Suitability of trachealis preparation for the present study

Unlike in striated muscle, the amount of thin/thick filament overlap in smooth muscle cannot be measured directly. However, if the sliding-filament/crossbridge mechanism is responsible for smooth muscle contraction, force generated by the muscle must be related to the degree of contractile filament overlap, which in turn must be related to the cell length. One place that allows us to examine the relationship among muscle cell length, filament overlap, and contractile force is at the plateau of an isotonic (constant load) contraction. During an isotonic contraction, shortening will occur as long as the muscle is capable of generating force greater than the isotonic load. Muscle shortening will eventually lead to a decrease in the amount of overlap between the thin and thick filaments and thus a decrease in the force generated by the muscle. Shortening will stop when the static force generated by the muscle equals the externally applied load, at the plateau of an isotonic contraction. This is true only when the orientations of individual muscle fibers (and the contractile filaments within) remain parallel to one another during shortening and that there is no internal load. From examining micrographs such as that shown (Fig. 1), it is clear that in trachealis preparations the cells all lie parallel to their longitudinal axes that are also parallel to the axis of force transmission. In a previous study (Kuo and Seow, 2004) we have shown that within a bundle of trachealis cells the contractile filaments also lie parallel to the longitudinal cell axes and the axis of force transmission. The tracheal smooth muscle preparation therefore is ideal for examining the length-force relationship, and a possible extension of the relationship to include the amount of contractile filament overlap, if excessive shortening (where the cell axes and the filament orientation may not remain parallel, and the internal load may not be negligible) is avoided.

Smooth muscle contractile unit

The most essential components that make up sarcomeres in striated muscle are the myosin (thick) filaments, the actin (thin) filaments and the Z-disks. The counterparts of these components are present in smooth muscle, albeit in variant forms. The dense bodies in smooth muscle are thought to be equivalent to Z-disks in the sense that they are anchoring

bodies for thin filaments (Bond and Somlyo, 1982). Smooth muscle thick filaments are probably side-polar (Small, 1977; Cooke et al., 1987; Xu et al., 1996; Tonino et al., 2002), or row-polar (Hinssen et al., 1978), in contrast to the bipolar variety found in striated muscle. A contractile unit in smooth muscle therefore is probably different from a sarcomere in terms of its functional mechanism and how it is assembled. It was structural evidence (Fig. 4) that led us to propose the model of contractile unit (Fig. 3). The model is different from those proposed previously (Hodgkinson et al., 1995; Schellenberg and Seow, 2003) in that predictions regarding mechanical behavior can be derived from geometric considerations of the model, as elaborated below.

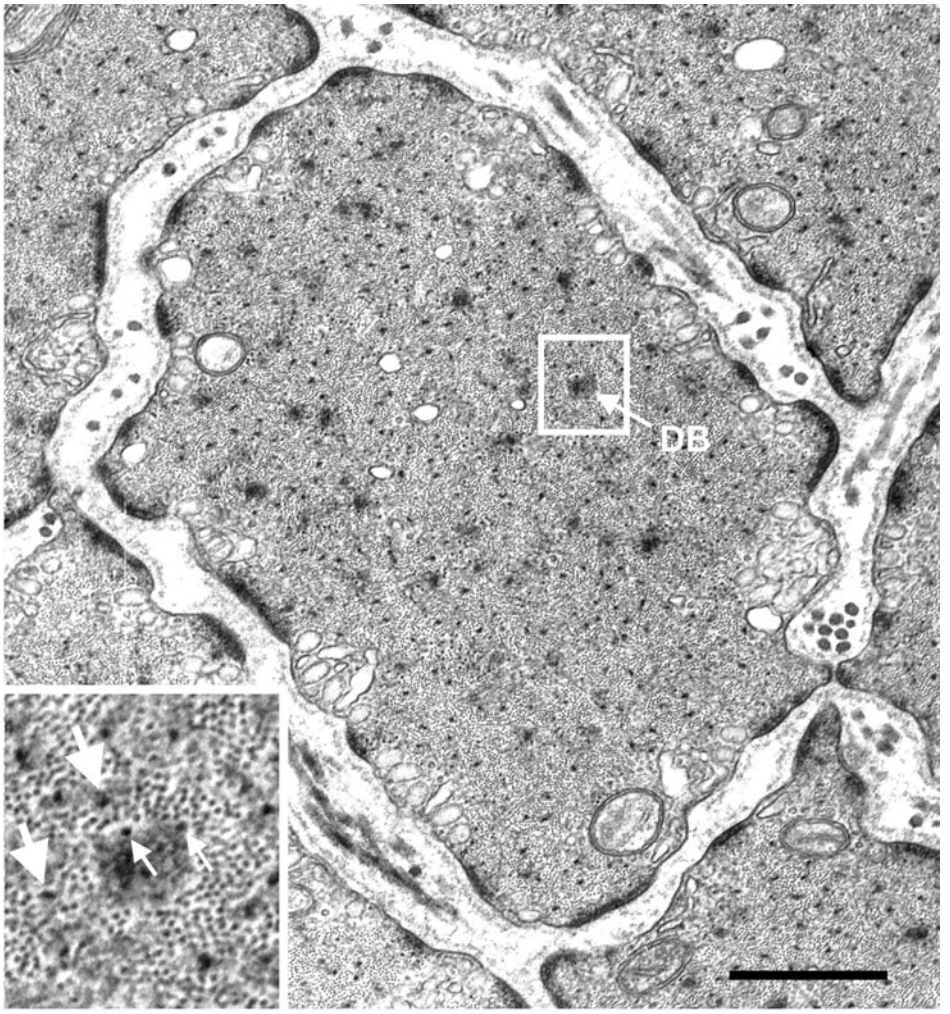

Fig. 5. Electron micrograph of a transverse section of porcine trachealis fixed at the in situ length and in the relaxed state. DB: dense body. The magnified portion shows a dense body surrounded by numerous thin filaments, intermediate filaments (small arrows) and thick filaments (large arrows). Bar, 1 μm.

Relationship between load on muscle and the amount of shortening

At the plateau of an isotonic contraction where the muscle is maximally contracted, force generated by the muscle equals the sum of all loads on the muscle. The loads include the externally applied isotonic load and the internal load that may stem from distortion of extracellular matrix and cytoskeleton due to shortening (Bramley et al., 1995; Meiss, 1999). The static mechanical equilibrium at the plateau of contraction (where shortening velocity is zero) offers an opportunity to examine the ability of a muscle to generate force at different lengths. If we assume that the structure of a contractile unit in smooth muscle resembles a sarcomere and if we also assume that the in situ length of the trachealis muscle is within the plateau portion of the muscle's length-force curve, shortening of the muscle within the plateau length range will not change the maximal overlap between the thick and thin filaments and therefore it will not diminish the ability of the muscle to generate force. (It is important to distinguish this force plateau from the identical forces obtained at different lengths after length adaptation. The subject of length adaptation will be discussed later). The amount of shortening will become load dependent when the muscle is operating on the ascending limb of its length-force curve. The present data on the length-force relationship of trachealis muscle cannot be explained by a sarcomere-like contractile unit because of the absence of force plateau (Fig. 2). Attempts to find the plateau in the present study by setting the same muscle to different initial lengths (Fig. 7) also failed. Our finding indicated that no matter what the starting length was, the ability of the muscle to carry load was diminished as soon as the muscle shortened. Furthermore, the length-force relationship was linear regardless of the starting length. These observations suggest that it is highly unlikely that myosin filaments of smooth muscle are bipolar and with a central bare zone. This has led us to consider the model presented in Fig. 3A. A variant form of the model is that the thick filament does not overlap the thin filaments completely within the contractile unit. The existence of non-overlap zones however could lead to a force plateau in the length-force relationship. To be consistent with the present finding of linear length-force relationship without a plateau (regardless of the starting length), we have to assume that thick filaments span the whole contractile-unit length (bracketed by the dense bodies), and that there is no non-overlap zones in between the dense bodies in a normal (fully adapted) contractile unit (Fig. 3A). A crucial assumption made here is that during an active isotonic contraction (with a duration measured in seconds) there is minimal ongoing length adaptation that could substantially alter the length-dependent ability of the muscle to generate force, so that the linear length-

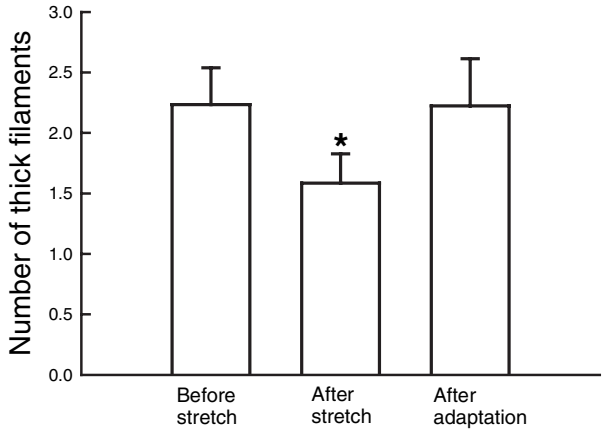

Fig. 6. The number of thick filaments within a 60-nm perimeter surrounding the edge of dense bodies measured (in micrographs such as that shown in Fig. 5) before and after a 30%-$L_{in\ situ}$ length increase was imposed on the muscle. The decrease in number (mean±s.e.m.) immediately after the stretch is statistically significant (*, $P<0.05$). After adaptation at the stretched length, the number returned to the pre-stretch level.

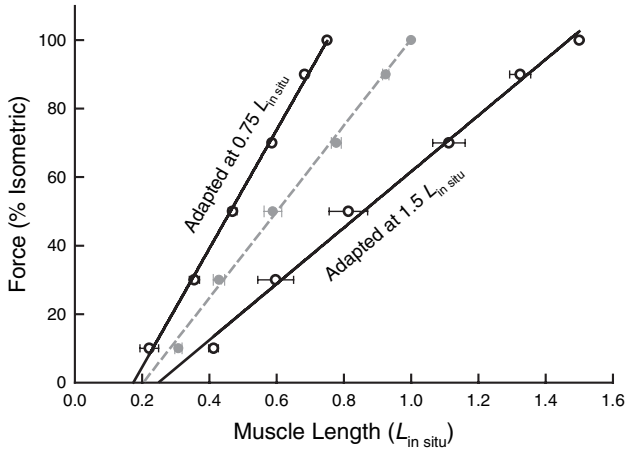

Fig. 7. Length-force relationships of trachealis preparations obtained at two adapted lengths. The data and fitted line (dashed) shown in gray depict the length-force relationship at $L_{in\ situ}$ (from Fig. 2), and are shown here as a reference. The isotonic loads are expressed as a percentage of F_{max}. The maximally shortened lengths at the various loads are normalized to $L_{in\ situ}$.

force relationship simply reflects the amount of contractile filament overlap. Gunst and colleagues (Gunst et al., 1995) have shown that changing the length of a relaxed muscle allows some degree of length adaptation that results in greater force generation in the subsequent isometric contraction, compared to force generated by an activated muscle that undergoes the same length change. Their results suggest that once fully activated, a muscle is less able to adapt to length change.

Shortening occurring near the in situ length probably encounters very little internal load stemming from distortion of extracellular matrix and cytoskeleton. The model of Fig. 3B predicts a linear relationship between external load and the

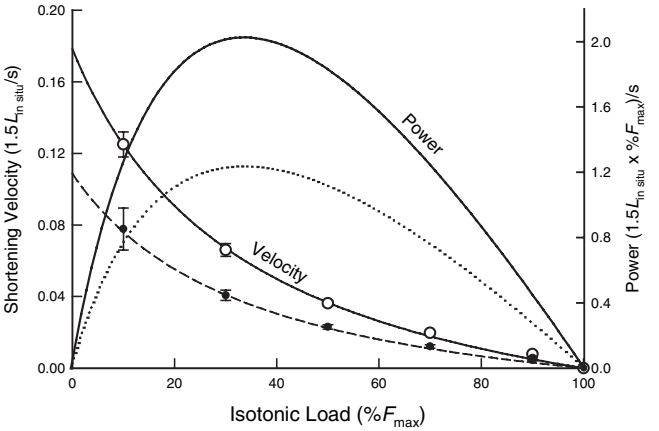

Fig. 8. Force-velocity and force-power relationships of trachealis preparations obtained at 0.75 $L_{in\ situ}$ (dashed curves) and at 1.5 $L_{in\ situ}$ (solid curves). See text for curve fitting.

amount of shortening near $L_{in\ situ}$. However, the linear relationship could be changed if increasing internal loads were encountered at shorter lengths. That is, the amount of shortening would be less than that predicted by the linear line at low (external) loads (Fig. 2). It is therefore surprising to us that a curvilinear length-force relationship was not found in shortening trachealis. There are several possible explanations: (1) The internal load has a linear relationship with muscle length; (2) force generated by the muscle is a non-linear function of muscle length, which when combined with a non-linear internal load produces a linear overall length-force relationship; (3) the internal load is negligible at muscle lengths greater than 20% $L_{in\ situ}$. The first possibility is not likely because if an internal load is present in our preparation, it is likely to be non-linearly related to the muscle length, as demonstrated in a similar preparation (Meiss and Pidaparti, 2004; Meiss and Pidaparti, 2005). The second possibility is also unlikely, because, even if by coincidence a linear relationship is produced by a combination of two non-linear components, the chance of this happening at three different initial lengths (Fig. 7) is extremely small. That leaves the third possibility as a likely explanation. Meiss and Pidaparti (Meiss and Pidaparti, 2005) found no evidence of internal load as long as their trachealis preparations did not shorten by more than 50%. In swine carotid artery, others (Walmsley and Murphy, 1987) found that although the average orientation of smooth muscle cells remained parallel to the long axis of the tissue at all lengths, the absolute value of angular deviations increased with shortening, and they calculated that the average decrease in force-generating capacity attributed to increasing smooth muscle and myofilament angular deviations was 7% when the preparation was shortened by 40%. Although the arterial preparations are very different from the tracheal preparations, their results suggest that some of the force decrease due to muscle shortening observed here could stem from myofilament angular deviations. This however does not explain the bulk of force decrease due to shortening and the linear relationship between muscle length and force. Pure muscle bundles can be dissected from a trachea; the use of this preparation (with any visible connective tissues removed under a 40× dissecting microscope) in the present study may be the reason we did not

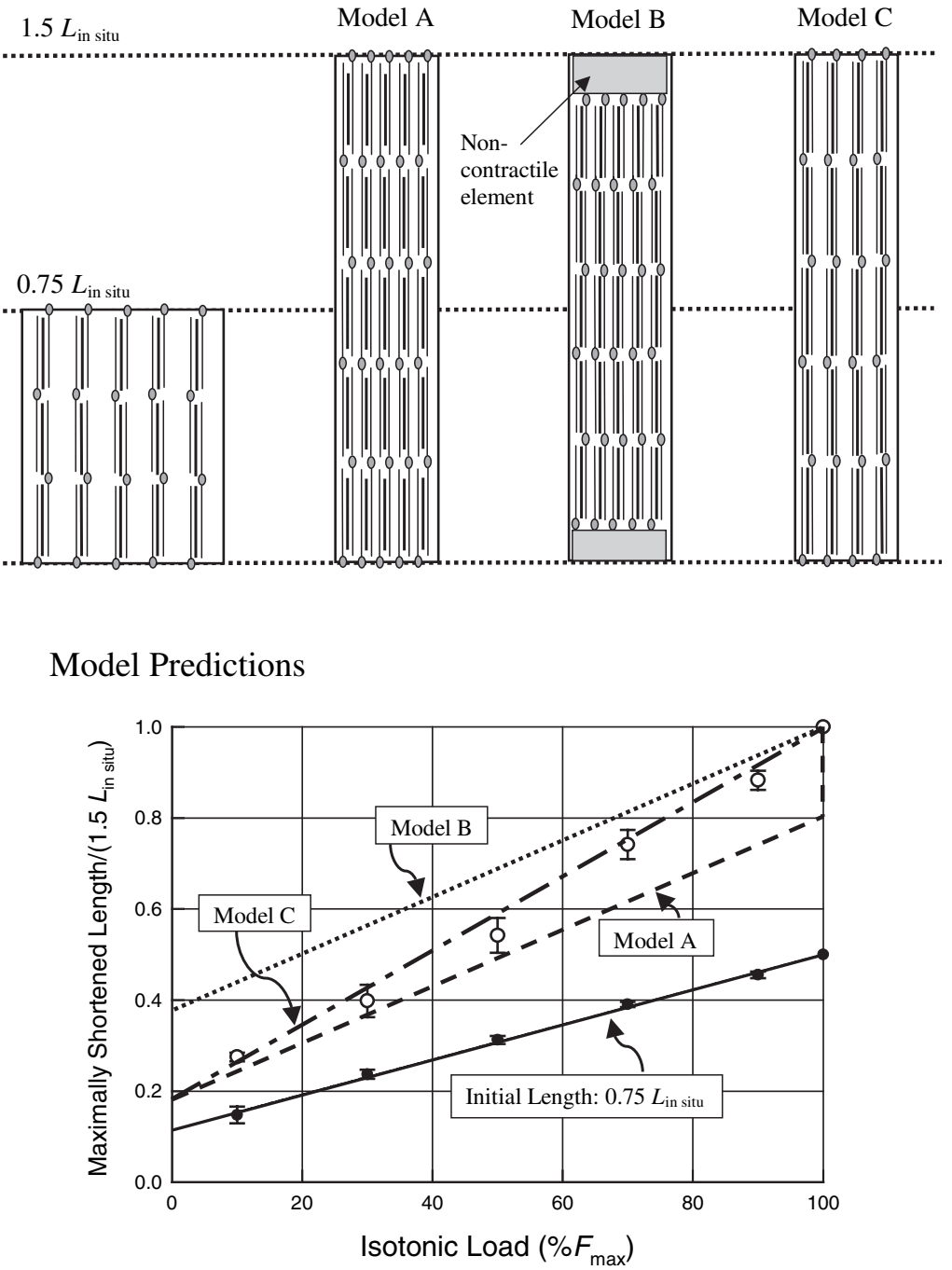

Fig. 9. Upper panel: Schematic representation of a trachealis cell and the intracellular arrangement of contractile units at 0.75 $L_{in\ situ}$ (left-hand rectangle), and the three possible rearrangements of the contractile units after the cell has been stretched and fully adapted at 1.5 $L_{in\ situ}$. Assuming that the kinetics of actomyosin crossbridge interaction are not affected by the contractile unit reconfiguration, all three models predict no change in isometric force with length doubling; all three models also predict an increase of 67% in shortening velocity, muscle power output, rate of ATP consumption and myosin thick filament density with length doubling [consistent with observations made by Kuo et al. (Kuo et al., 2003), and data in Fig. 8]. In all models, the number of contractile units in series has increased by 67% with length doubling. In Model A, the increase in cell length is associated with the appearance of non-overlap zones between the thick and thin filaments, and no change in the thick filament length. In Model B, the increase in cell length is associated with the appearance of non-contractile elements (instead of non-overlap zones) in series with the contractile units, and no change in the thick filament length. Although the non-contractile elements are placed at the ends of the cell in the drawing, they can be anywhere in the cell as long as they are in series with the contractile units. In Model C, the increase in cell length creates neither non-overlap zones nor non-contractile elements; instead, the thick filament length is increased by 20% and the number of contractile units in parallel decreased by 20%. Lower panel: Predictions by the models regarding the relationship between maximally shortened length and isotonic load. The data points are redrawn from Fig. 7. The model predictions are based on the linear regression line (solid) for the data collected at 0.75 $L_{in\ situ}$. The maximally shortened length under zero-load is assumed proportional to the number of dense bodies in series plus any serially connected non-contractile elements.

detect a significant amount of internal load even at short muscle lengths.

The model presented in Fig. 3 appears to be the simplest that can accommodate the data collected in the present study (Figs 2 and 7). The requirement that a thick filament spans the whole length of a contractile unit stems from the observation that a small amount of shortening of the muscle resulted in a decrease in the force generated by the muscle (Figs 2 and 7). If there were gaps between the thick filament and the dense bodies, the initial shortening of the contractile unit would result in the narrowing of these gaps at no cost to the force generating capability. Another requirement of the model is that only the portion of the thick filament between the dense bodies that overlaps with thin filaments (solid portion of the thick filament depicted in Fig. 3) is able to generate force; as the thick filament slides over and passes the dense bodies (white portions of thick filament depicted in Fig. 3) it loses its ability to generate force, perhaps because there are no nearby actin

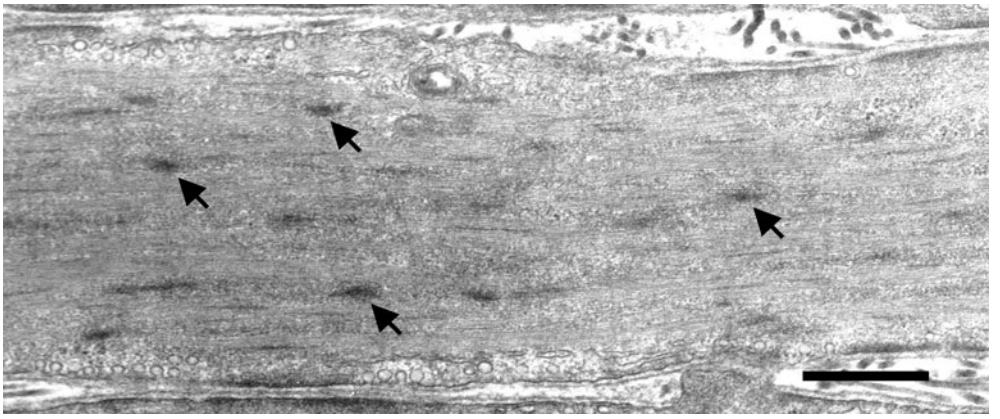

Fig. 10. Electron micrograph (longitudinal section) of a trachealis cell showing dense bodies (arrows). The muscle was fixed at 1.5 $L_{in\ situ}$ in the relaxed state. Bar, 1 μm.

filaments with the 'correct' polarity available for interaction. The simplicity of the model lies in the mechanism that links the amount of filament overlap (or force-generating ability) to the instantaneous length of the muscle in a direct and linear fashion, and straightforwardly accommodates the present data.

Muscle shortening and morphological change after a quick stretch

The sliding-filament mechanism similar to that found in striated muscle has never been clearly demonstrated in intact smooth muscle. If such a mechanism exists in smooth muscle, isotonic shortening with or without a preceding stretch will arrive at the same final length (where the muscle is maximally shortened under the same load), as graphically illustrated (Fig. 3C). The quick stretch from $L_{in\ situ}$ in the relaxed state appears to increase the distance between dense bodies in contractile units and to cause sliding of the thin filaments relative to the thick filaments. The amount of shortening in the subsequent isotonic contraction, as a result, has increased by exactly the amount of stretch (Fig. 2).

Another line of evidence supporting the sliding filament model came from morphological observations that the thick filament density surrounding the dense bodies in transverse thin sections decreased immediately after a quick stretch (Fig. 6). The observation suggests that the stretch probably pulled the dense bodies away from the ends of their accompanying thick filaments.

The model presented in Fig. 3 lacks some quantitative information. For example, the thick and thin filament lengths are not specified. There is a wide range of estimated thick filament length in smooth muscle, from 1.6 to 8 μm (Ashton et al., 1975; Small, 1977; Small et al., 1990). Thin filament length appears to be just as variable, from 1.35 (Drew and Murphy, 1997) to 4.5 μm (Small et al., 1990). The variability suggests that there may not be a fixed length for the filaments. There is evidence suggesting that contractile filaments lengthen during activation (Gillis et al., 1988; Mehta and Gunst, 1999; Seow et al., 2000; Herrera et al., 2002), and in adaptation to a longer cell length (Kuo et al., 2003; Herrera et al., 2004). The extent of filament length variability under different conditions may also depend on smooth muscle types (Gillis et al., 1988). These factors probably contribute to the large range of estimates of the filament lengths and the fact that we do not have a consensus on the measurements. If we assume that the

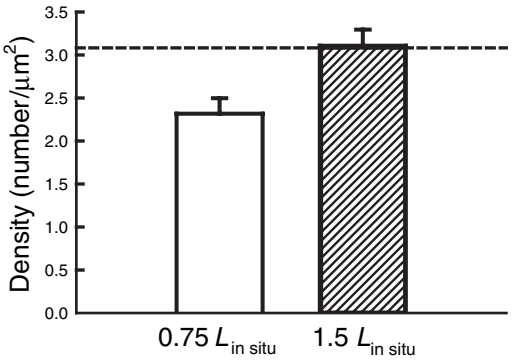

Fig. 11. Density of dense bodies measured from 4-μm cell longitudinal sections in micrographs such as that shown in Fig. 10. The dashed line indicates an increase of 33% from the average value measured at 0.75 $L_{in\ situ}$.

thin filaments are not much longer than the thick filaments, according to the model shown in Fig. 3, a sufficiently large stretch will reduce the amount of overlap between the thin and thick filaments (Fig. 3C). This could account for some of the isometric force decrease seen immediately after a quick stretch (Fig. 2). Another cause for the decrease could be the mechanical perturbation associated with the length change, as our previous studies have shown that the unphosphorylated thick filaments are labile and could be induced to depolymerise by mechanical agitation (Kuo et al., 2001). Oscillatory loading of actively shortened tracheal preparation has also been shown to reduce the ability of the muscle to shorten (Fredberg et al., 1999; Dowell et al., 2005) owing to perturbation-induced interference in the actomyosin interaction, and perhaps alteration in ultrastructure of the contractile filaments. To predict accurately the slope and other features of the descending limb of the length-force curve from models such as that in Fig. 3, we need quantitative information regarding the thick and thin filament lengths, before and after the muscle is subjected to a length change. Unfortunately, the information is not available at present.

Adaptation of smooth muscle to different lengths

Many aspects of the muscle behavior described in this study are related to the adaptive response of tracheal smooth muscle

to changes in cell length. It appears that the muscle has an innate tendency to optimize the contractile filament overlap at any cell length within its physiological range and to maintain the ability to generate maximal force over that length range (Pratusevich et al., 1995; Gunst et al., 1995; Kuo et al., 2003) (see Fig. 7). With a twofold change in length, the maximal isometric force produced by the muscle (fully adapted at each length) was not different. The shortening velocity, on the other hand, was higher for the muscle adapted at the longer cell length (Fig. 8). These findings are essentially the same as those found earlier (Pratusevich et al., 1995) and could be interpreted by a simple model where plastic adaptation alters the number of contractile units in series within a cell (Kuo et al., 2003; Lambert et al., 2004). Some specific features of the models proposed in this study were not considered in our previously proposed models, because of the lack of data at that time. For example, the requirement that thick filaments span the entire length of the contractile unit was not specified by Kuo et al. (Kuo et al., 2003) and they did not treat the number of contractile units in parallel as a variable. Data presented in Figs 7, 8 and 11 have provided us with further functional and structural information and allowed us to put additional constraints on the models that we have developed earlier. The three possible rearrangements of contractile units within a cell which has undergone a doubling in cell length, cannot be distinguished in our previous studies: they all predict no change in isometric force, and 5/3 or 1.67-fold increase in shortening velocity, muscle power output, rate of ATP consumption and myosin filament density (in transverse cell sections). These predictions were all confirmed by Kuo et al. (Kuo et al., 2003). With the new data presented in Figs 7 and 11, we are now able to propose a more specific model. Model C appears to be the 'correct' model in that it gives a good fit to all the available data (Fig. 9). One prediction derived from Model C is that the dense body density will increase by 33% with length doubling. (Models A and B both predict a 67% increase with the same length change). The change in dense body density measured in longitudinal sections (Fig. 11) is consistent with that predicted by Model C. Because the cell volume of trachealis is constant at different cell lengths (Kuo et al., 2003), doubling the cell length reduces the cell cross section by half. This will bring the dense bodies closer together and contribute to the observed increase in dense body density in longitudinal thin sections. This effect, however, is cancelled by the tendency of the dense bodies to move out of the sampling window (the 4-μm longitudinal section) owing to the length increase. It should be pointed out that morphologically dense bodies are nonhomogeneous in size. We only counted the number of discrete dense bodies; their size was not taken into consideration. The distribution of dense bodies was also inhomogeneous; often there were large cytoplasmic areas containing thin and thick filaments, but not dense bodies (at least not in their usual appearance). It is possible that the functional dense bodies depicted in our models and the dense bodies identified morphometrically are not exactly the same thing, but somehow they are correlated.

It appears, therefore, that length adaptation involves changes in the number of contractile units in series and in parallel. Furthermore, the thick filament length is variable and is determined by the thin filament lattice bounded by the dense bodies (Fig. 9, Model C). This conclusion is consistent with the finding by Sobieszek (Sobieszek, 1972) that myosin filament length could be altered by adding or subtracting myosin dimers at the two 'smooth' surfaces at the tapered ends of the filament. There appears to be no internal mechanism for limiting the filament growth, regulation of filament length therefore has to be controlled by external factors, such as the dimension of the thin filament lattice.

Functional implications of smooth muscle length adaptation

An interesting observation (and model prediction) is that the maximally shortened length at any load was always shorter in muscles adapted at a shorter length (Fig. 7). This unique smooth muscle property may have important clinical implications. Excessive shortening of airway smooth muscle is implicated in the disease of asthma (King et al., 1999). Alterations in extracellular environment (due to airway inflammation and inflammation-associated tissue injury and repair, for example) that result in adaptation of smooth muscle cells at abnormally short lengths (and the subsequent regaining of contractility at the short length that leads to further shortening) could underlie the pathology of asthma. Similar speculations can be extended to other smooth muscle-related organ dysfunction where exaggerated shortening of smooth muscle is the root problem.

Special thanks to Pitt Meadows Meats (Pitt Meadows, BC) for the supply of fresh porcine tracheas in kind support for this research project. In particular, we would like to thank Cathy Pollock, Inspector in Charge, Canada Food Inspection Agency (Establishment # 362) for her help in obtaining the tracheas. B.E.M. is supported by a fellowship from the Michael Smith Foundation for Health Research. C.Y.S. is a CIHR/BC Lung Association Investigator. This study was supported by operating grants from the Canadian Institutes of Health Research (MT-13271, MT-4725).

References

Ashton, F. T., Somlyo, A. V. and Somlyo, A. P. (1975). The contractile apparatus of vascular smooth muscle: intermediate high voltage stereo electron microscopy. *J. Mol. Biol.* **98**, 17-29.

Bond, M. and Somlyo, A. V. (1982). Dense bodies and actin polarity in vertebrate smooth muscle. *J. Cell Biol.* **95**, 403-413.

Bramley, A. M., Roberts, C. R. and Schellenberg, R. R. (1995). Collagenase increases shortening of human bronchial smooth muscle in vitro. *Am. J. Respir. Crit. Care Med.* **152**, 1513-1517.

Cooke, P. H., Kargacin, G., Craig, R., Fogarty, K. and Fay, F. S. (1987). Molecular structure and organization of filaments in single, skinned smooth muscle cells. In *Regulation and Contraction in Smooth Muscle* (ed. M. J. Siegman, A. P. Somlyo and N. L. Stephens), pp. 1-25. New York: Alan R. Liss.

Dillon, P. F., Aksoy, M. O., Driska, S. P. and Murphy, R. A. (1981). Myosin phosphorylation and the cross-bridge cycle in arterial smooth muscle. *Science* **211**, 495-497.

Dowell, M. L., Lakser, O. J., Gerthoffer, W. T., Fredberg, J. J., Stelmack, G. L., Halayko, A. J., Solway, J. and Mitchell, R. W. (2005). Latrunculin B increases force fluctuation-induced relengthening of ACh-contracted, isotonically shortened canine tracheal smooth muscle. *J. Appl. Physiol.* **98**, 489-497.

Drew, J. S. and Murphy, R. A. (1997). Actin isoform expression, cellular heterogeneity, and contractile function in smooth muscle. *Can. J. Physiol. Pharmacol.* **75**, 869-877.

Fredberg, J. J., Inouye, D. S., Mijailovich, S. M. and Butler, J. P. (1999). Perturbed equilibrium of myosin binding in airway smooth muscle and its implications in bronchospasm. *Am. J. Respir. Crit. Care Med.* **159**, 959-967.

Gillis, J. M., Cao, M. L. and Godfraind-De Becker, A. (1988). Density of

myosin filaments in the rat anococcygeus muscle, at rest and in contraction. II. *J. Muscle Res. Cell Motil.* **9**, 18-29.

Gordon, A. M., Huxley, A. F. and Julian, F. J. (1966). The variation in isometric tension with sarcomere length in vertebrate muscle fibres. *J. Physiol.* **184**, 170-192.

Guilford, W. H. and Warshaw, D. M. (1998). The molecular mechanics of smooth muscle myosin. *Comp. Biochem. Physiol. B Biochem. Mol. Biol.* **119**, 451-458.

Gunst, S. J., Meiss, R. A., Wu, M. F. and Rowe, M. (1995). Mechanisms for the mechanical plasticity of tracheal smooth muscle. *Am. J. Physiol.* **268**, C1267-C1276.

Hanson, J. and Huxley, H. E. (1953). Structural basis of the cross-striations in muscle. *Nature* **172**, 530-532.

Herrera, A. M., Kuo, K. H. and Seow, C. Y. (2002). Influence of calcium on myosin thick filament formation in intact airway smooth muscle. *Am. J. Physiol.* **282**, C310-C316.

Herrera, A. M., Martinez, E. C. and Seow, C. Y. (2004). Electron microscopic study of actin polymerization in airway smooth muscle. *Am. J. Physiol.* **286**, L1161-L1168.

Hill, A. V. (1938). The heat of shortening and the dynamic constants of muscle. *Proc. R. Soc. London Series B* **126**, 136-195.

Hinssen, H., D'Haese, J., Small, J. V. and Sobieszek, A. (1978). Mode of filament assembly of myosins from muscle and nonmuscle cells. *J. Ultrastruct. Res.* **64**, 282-302.

Hodgkinson J. L., Newman, T. M., Marston, S. B. and Severs, N. J. (1995). The structure of the contractile apparatus in ultrarapid frozen smooth muscle: Freeze fracture, deep-etch, and freeze-substitution studies. *J. Struct. Biol.* **114**, 93-104.

Huxley, A. F. (1957). Muscle structure and theories of contraction. *Prog. Biophys. Biop. Ch.* **7**, 255-318.

Huxley, A. F. and Niedergerke, R. (1954). Structural changes in muscle during contraction; interference microscopy of living muscle fibres. *Nature* **173**, 971-973.

King, G. G., Paré, P. D. and Seow, C. Y. (1999). The mechanics of exaggerated airway narrowing in asthma: the role of smooth muscle. *Respir. Physiol.* **118**, 1-13.

Kuo, K.-H. and Seow, C. Y. (2004). Contractile filament architecture and force transmission in swine airway smooth muscle. *J. Cell Sci.* **117**, 1503-1511.

Kuo, K.-H., Wang, L., Paré, P. D., Ford, L. E. and Seow, C. Y. (2001). Myosin thick filament lability induced by mechanical strain in airway smooth muscle. *J. Appl. Physiol.* **90**, 1811-1816.

Kuo, K.-H., Herrera, A. M., Wang, L., Paré, P. D., Ford, L. E., Stephens, N. L. and Seow, C. Y. (2003). Structure-function correlation in airway smooth muscle adapted to different lengths. *Am. J. Physiol.* **285**, C384-C390.

Lambert, R. K., Paré, P. D. and Seow, C. Y. (2004). Mathematical description of geometric and kinematic aspects of smooth muscle plasticity and some related morphometrics. *J. Appl. Physiol.* **96**, 469-476.

Mehta, D. and Gunst, S. J. (1999). Actin polymerization stimulated by contractile activation regulates force development in canine tracheal smooth muscle. *J. Physiol.* **519**, 829-840.

Meiss, R. A. (1999). Influence of intercellular tissue connections on airway muscle mechanics. *J. Appl. Physiol.* **86**, 5-15.

Meiss, R. A. and Pidaparti, R. M. (2004). Mechanical state of airway smooth muscle at very short lengths. *J. Appl. Physiol.* **96**, 655-667.

Meiss, R. A. and Pidaparti, R. M. (2005). Active and passive components in the length-dependent stiffness of tracheal smooth muscle during isotonic shortening. *J. Appl. Physiol.* **98**, 234-241.

Pratusevich, V. R., Seow, C. Y. and Ford, L. E. (1995). Plasticity in canine airway smooth muscle. *J. Gen. Physiol.* **105**, 73-79.

Qi, D., Mitchell, R. W., Burdyga, T., Ford, L. E., Kuo, K.-H. and Seow, C. Y. (2002). Myosin light chain phosphorylation facilitates in vivo myosin filament reassembly after mechanical perturbation. *Am. J. Physiol.* **282**, C1298-C1305.

Schellenberg, R. R. and Seow, C. Y. (2003). Airway smooth muscle and related extracellular matrix in normal and asthmatic lung. In *Middleton's Allergy: Principles and Practice* (6th Edition) (ed. N. F. Adkinson, Jr, J. W. Yunginger, W. W. Busse, B. S. Bochner, S. T. Holgate and F. E. R. Simons), pp. 711-725. Philadelphia: Mosby.

Seow, C. Y. and Stephens, N. L. (1986). Force-velocity curves for smooth muscle: analysis of internal factors reducing velocity. *Am. J. Physiol.* **251**, C362-C368.

Seow, C. Y., Pratusevich, V. R. and Ford, L. E. (2000). Series-to-parallel transition in the filament lattice of airway smooth muscle. *J. Appl. Physiol.* **89**, 869-876.

Small, J. V. (1977). Studies on isolated smooth muscle cells. The contractile apparatus. *J. Cell Sci.* **24**, 327-349.

Small, J. V., Herzog, M., Barth, M. and Draeger, A. (1990). Supercontracted state of vertebrate smooth muscle cell fragments reveals myofilament lengths. *J. Cell Biol.* **111**, 2451-2461.

Sobieszek A. (1972). Cross-bridges on self-assembled smooth muscle myosin filaments. *J. Mol. Biol.* **70**, 741-744.

Tonino, P., Simon, M. and Craig, R. (2002). Mass determination of native smooth muscle myosin filaments by scanning transmission electron microscopy. *J. Mol. Biol.* **318**, 999-1007.

Uvelius, B. (1976). Isometric and isotonic length-tension relations and variations in cell length in longitudinal smooth muscle from rabbit urinary bladder. *Acta Physiol. Scand.* **97**, 1-12.

Walmsley, J. G. and Murphy, R. A. (1987). Force-length dependence of arterial lamellar, smooth muscle, and myofilament orientations. *Am. J. Physiol.* **253**, H1141-H1147.

Xu, J. Q., Harder, B. A., Uman, P. and Craig, R. (1996). Myosin filament structure in vertebrate smooth muscle. *J. Cell Biol.* **134**, 53-66.